LA-UR-97-1915

C.3

Title: Rossi-α Measurements in the Fast Critical Assembly XIX-2

Author(s): Gregory D. Spriggs (LANL)
Takeshi Sakurai (JAERI)
Shigeaki Okajima (JAERI)

Submitted to: Distribution

June 16, 1997

Los Alamos
NATIONAL LABORATORY

Rossi-α Measurements in the Fast Critical Assembly XIX-2

Gregory D. Spriggs
Los Alamos National Laboratory, P.O. Box 1663, MS B226, Los Alamos, NM 87545-001

Takeshi Sakurai
Japan Atomic Energy Research Institute, Tokai-mura, Naka-gun, Ibaraki-ken 319-11, Japan

Shigeaki Okajima
Japan Atomic Energy Research Institute, Tokai-mura, Naka-gun, Ibaraki-ken 319-11, Japan

Abstract – *A Rossi-α experiment was performed on the zero-power, XIX-2 assembly at the Fast Critical Assembly (FCA) facility operated by the Japan Atomic Energy Research Institute (JAERI), Tokai-mura, Japan. The XIX-2 assembly is a plutonium/natural uranium system comprised of a plutonium/natural uranium core surrounded by a depleted uranium dioxide blanket (referred to as the soft blanket). The soft blanket is surrounded by an outer blanket comprised of depleted uranium metal (referred to as the depleted blanket). Because the neutron lifetime in the soft and depleted blankets are significantly larger than the neutron lifetime in the core region, multiple decay modes were observed during this experiment. The first decay mode was measured with reasonable accuracy; however, because of the high intrinsic source strength produced by the large amounts of Pu-240 contained in the core region, the intrinsic source background was reached very rapidly, thus precluding the second decay mode from being resolved well enough to estimate the average system lifetime. Nevertheless, using the first decay mode (i.e., the rapid die-away time constant), the alpha at delayed critical for this root was measured to be 13,100 +/- 134 s^{-1}. This root is associated with the prompt neutron lifetime of the core region. Using the calculated β_{eff} of 0.0036, the core lifetime is estimated to be 275 +/- 3% ns at delayed critical.*

I. INTRODUCTION

As part of an international project sponsored by the Nuclear Energy Agency (NEA), Organization of Economic Cooperation & Development (OECD), a Rossi-α experiment was performed on the zero-power, XIX-2 assembly at the Fast Critical Assembly (FCA) facility operated by the Japan Atomic Energy Research Institute (JAERI), Tokai-mura, Japan. The XIX-2 assembly is a multi-region system comprised of an inner core fueled with ^{239}Pu and natural-enrichment uranium. The core is surrounded by a depleted uranium dioxide blanket containing significant quantities of sodium (referred to as the soft blanket). The soft blanket is surrounded by an outer reflector comprised mainly of depleted uranium metal (referred to as the depleted blanket). Cross-sectional views of the core are shown in Figs. 1, 2, and 3 and the corresponding atom densities are given in Table I.

The intent of the Rossi-α experiment is to measure the alpha at delayed critical and also to measure the effective delayed neutron fraction at several subcritical configurations in the vicinity of delayed critical. (In this report, we only present the Rossi-α measurements; further analysis must be performed using the Rossi-α data in order to determine the value of β_{eff}. This will be presented in a subsequent version of this report.) From these two measured quantities, the effective

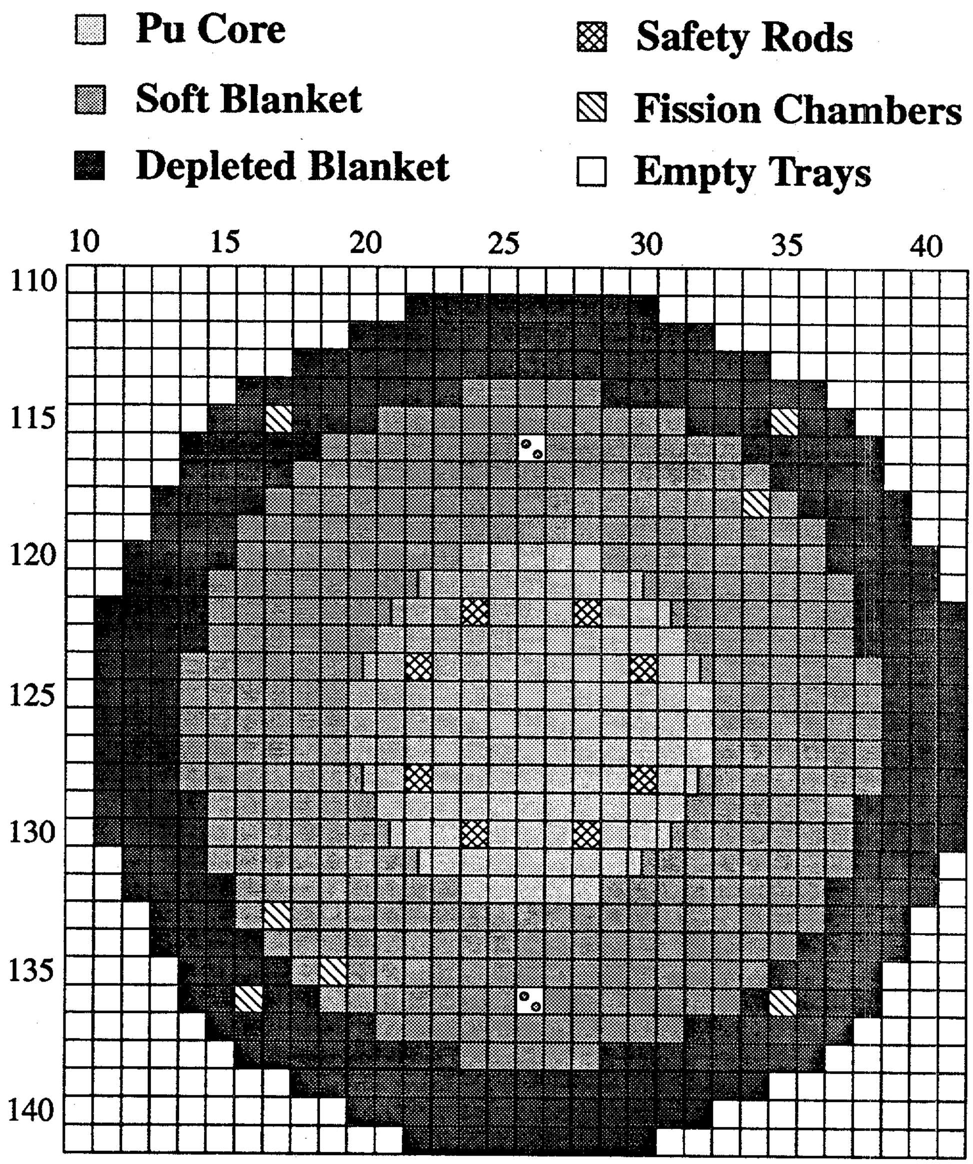

Fig1. Cross-sectional view of FCA XIX-2 assembly. Two pairs of He-3 detectors are located in positions 26-116 and 26-136.

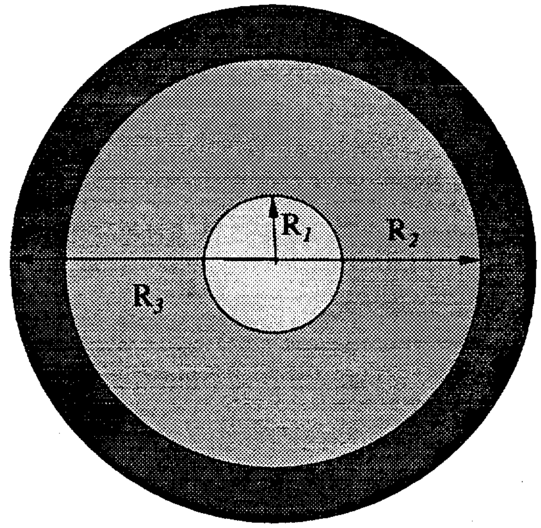

Figure 2. Effective radii of the three regions of the XIX-2 Assembly. $R_1 = 35.64$ cm, $R_2 = 68.30$ cm, $R_3 = 86.36$ cm.

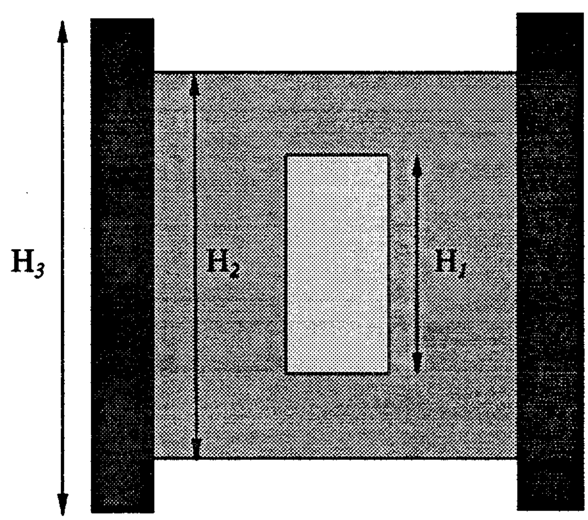

Figure 3. Effective diameters and heights of the three regions of the XIX-2 Assembly. $H_1 = 30.48$ cm, $H_2 = 60.96$ cm, $H_3 = 66.04$.

adjoint-weighted neutron lifetime of the system can be inferred. By comparing this measured lifetime to a calculated lifetime, one can then access the adequacy of the nuclear cross section set(s) used to perform the calculation. Previous comparisons of this type have shown that the absorption cross section of many of our most commonly used cross section sets are biased by 20 to 30% in both uranium and plutonium systems.

II. EXPERIMENT SETUP

Four ^{3}He detectors were placed in the soft blanket region of the XIX-2 core. Each detector had its own pre-amp, amplifier, and SCA output circuitry. The output from two of the detector systems were OR-ed (i.e., summed) together in a LeCroy "Logic Fan-in/Fan-out" unit (Model 429a) and then fed into Channel A of a Langley-Ford Model 1096 Correlator as a very narrow NIM logic pulse. The other two detectors were OR-ed together using the same fan-in/fan-out unit and then fed into Channel B of the correlator as the start signal. A synoptic diagram of the detector system is shown in Fig. 4.

Because of the relatively short life expectancy of a prompt-fission chain in the XIX-2 core and the relatively large deadtime inherent with ^{3}He detectors, the Langley-Ford Correlator was operated in the *cross correlation mode* (i.e., signal A was correlated against signal B). When operated in this mode, the vast majority of the deadtime effects usually encountered at the beginning of a Rossi-α curve are greatly reduced. This is particularly useful (and almost always necessary) when measuring Rossi-α curves in fast, complex systems in which the *core* lifetime is very small in comparison to the lifetime of a neutron in the surrounding blanket/reflector, such as in the XIX-2 assembly. This large difference in neutron lifetimes ultimately produces multiple decay modes—one that is very fast (which is associated with the lifetime of core neutrons) and one that is relatively slow (which is associated with the weighted average between the core and the blanket/reflector lifetimes). A significant detector deadtime can preclude the fast decay constant from being accurately measured, which can also effect the measurement of the slow decay constant.

Because the XIX-2 assembly is fueled with a large amount of plutonium, another special problem is encountered with the high intrinsic spontaneous source produced by ^{240}Pu. Even when the system is brought to source equilibrium at relatively large negative reactivities (0.9 to 0.95), the high intrinsic source strength will cause relatively large count rates in any high-efficiency detector placed within the system. As delayed critical is approached, the problem is further exacerbated; the count rates can become exceedingly high, causing the detector systems to *paralyze* in the reactivity regime where the Rossi-α experiment is best performed (i.e., in the vicinity of delayed critical). For this particular experiment, the high intrinsic source strength produced count rates in each ^{3}He detector on the order of 50,000 to 80,000 cps at approximately \$0.50 subcritical, which produced deadtimes in excess of 25%. When the system was brought to approximately \$0.25 subcritical, the detectors began to show definite signs of paralyzing; the count rates decreased rather than increased. Consequently, the alpha at delayed critical had to be determined by extrapolating alpha data in the reactivity range of -\$2.00 to -\$0.50, which, of course, yields a greater uncertainty in that measurement. Nevertheless, the uncertainty of the alpha at delayed critical for this experiment was shown to be on the order of 2% or less.

Table I. Atom Densities for XIX-2 Assembly ($x10^{24}$ atoms/cm^3)

	Core	Soft Blanket	Control Rods	Depleted Blanket
H	$7.7076x10^{-5}$		$1.3388x10^{-4}$	
^{10}B	$2.3314x10^{-7}$		$2.3314x10^{-7}$	
^{11}B	$8.4818x10^{-7}$		$8.4817x10^{-7}$	
C	$6.8773x10^{-5}$		$1.1645x10^{-4}$	
^{14}N	$6.8582x10^{-3}$		$6.8581x10^{-3}$	
O	$1.8164x10^{-4}$	$1.8350x10^{-2}$	$2.0624x10^{-4}$	
Na	$7.6564x10^{-3}$	$7.6564x10^{-3}$	$7.6563x10^{-3}$	
Al	$7.1583x10^{-3}$		$6.8583x10^{-3}$	
Si	$4.1088x10^{-5}$		$1.7455x10^{-6}$	
Cr	$3.6526x10^{-3}$	$3.1174x10^{-3}$	$4.2346x10^{-3}$	$1.8101x10^{-3}$
Mn	$2.7075x10^{-4}$	$2.2939x10^{-4}$	$3.0903x10^{-4}$	$1.2001x10^{-4}$
Fe	$1.3235x10^{-2}$	$1.1217x10^{-2}$	$1.5255x10^{-2}$	$6.4727x10^{-3}$
Ni	$1.6811x10^{-3}$	$1.4131x10^{-3}$	$1.9014x10^{-3}$	$7.8944x10^{-4}$
U^{235}	$5.3037x10^{-5}$	$1.8606x10^{-5}$	$2.7860x10^{-3}$	$8.4422x10^{-5}$
U^{238}	$7.3148x10^{-3}$	$9.1586x10^{-3}$	$6.9923x10^{-3}$	$4.0174x10^{-2}$
^{239}Pu	$2.0911x10^{-3}$			
^{240}Pu	$1.8270x10^{-4}$			
^{241}Pu	$5.6335x10^{-6}$			
^{242}Pu	$1.6074x10^{-6}$			
^{241}Am	$1.1669x10^{-5}$			

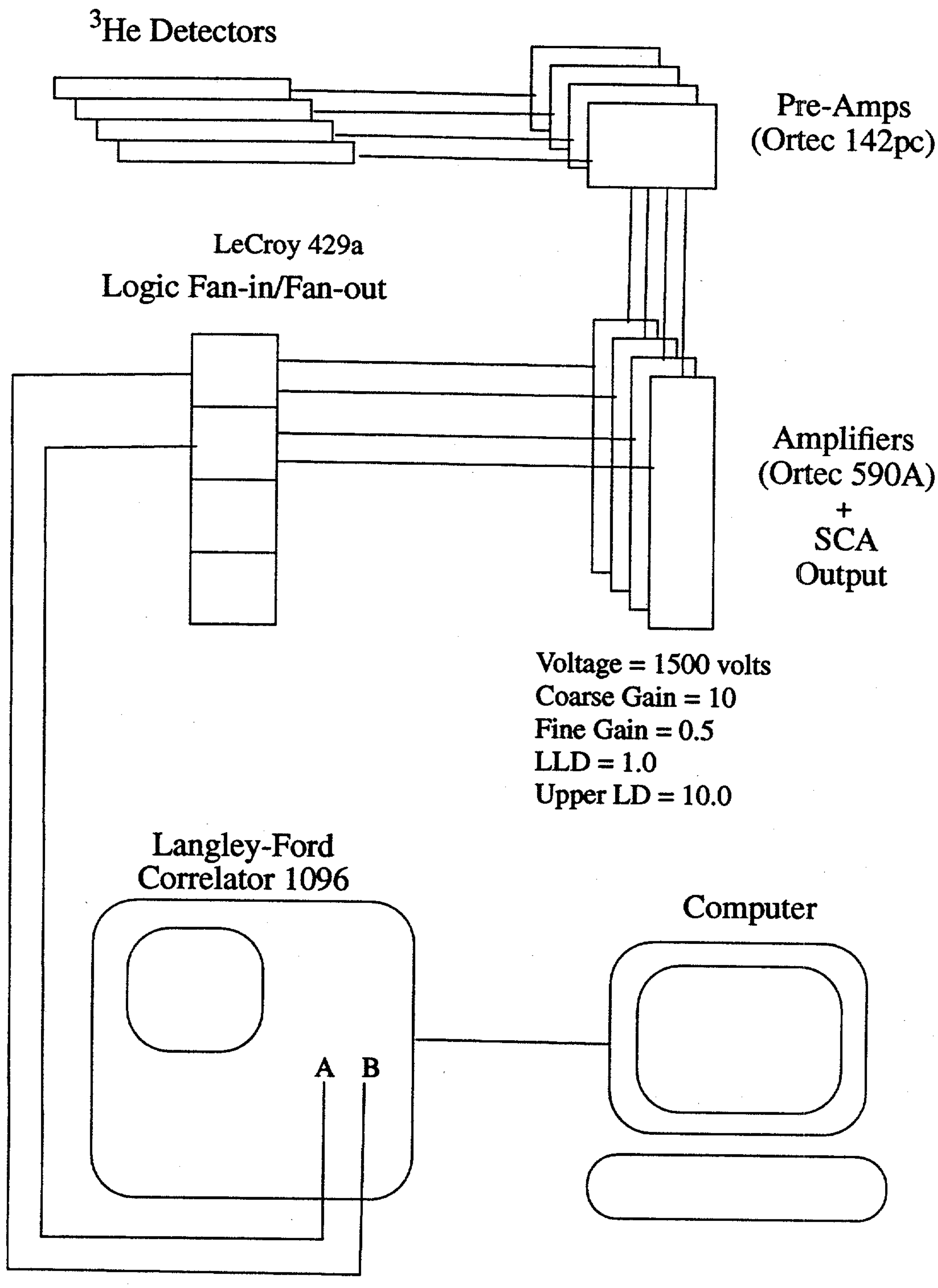

Fig. 4. Synoptic Diagram of Detector System and Data Acquisition Equipment.

III. EXPERIMENTAL RESULTS

Preliminary Measurements

A preliminary set of Rossi-α curves was measured to determine if the high detector deadtime would preclude an accurate measure of the die-away curves (see Appendix A, Figs. A-1 through A-7). In each of these preliminary measurements, we noted that at least two alphas were present, although, in most of the cases, the time scale for the preliminary runs was not properly set to accurately measure the second (i.e., the longer) decay constant.

As previously mentioned, when the XIX-2 assembly was operated in source equilibrium at approximately -\$0.25, it was noted that the ^{3}He detector systems were very nearly paralyzed. The count rate of both pairs of ^{3}He detectors decreased by a factor of two relative to the previous configuration at approximately \$0.52 subcritical. In order to determine if the alpha measurement at -\$0.25 was still good, the alphas obtained from the rapid die-away portion of each curve was plotted as a function of the inverse count rate as obtained by one of the low-efficiency fission chambers located in the depleted blanket (see Fig. 1). Extrapolating this function to zero allowed us to determine the alpha at delayed critical (see Fig. A-8), which then allowed us to determine the reactivity at each subcritical point in the series of measurements. Much to our pleasant surprise, the reactivities calculated in this fashion agreed to within a few cents of the reactivities obtained from a previous control rod calibration. Hence, from these preliminary results, we concluded that the alpha curves were not adversely affected by the large detector deadtime.

Final Results

Based on the aforementioned preliminary measurements, the time scale of each Rossi-α measurement was adjusted so that both decay constants could be measured accurately. Furthermore, to minimize the uncertainty associated with statistical fluctuations, it was also decided to run each Rossi-α for at least 5 hours. Unfortunately, because of time limitations of the experiment, only three subcritical configurations could be measured for this length of time (see Figs 5, 6, and 7).

An interesting effect was observed during these three measurements. Because of the high intrinsic source strength, the mean time between successive prompt-fission chains was very small, making it very difficult to observe long fission chains without those chains overlapping subsequent chains. As a consequence, the correlation curves followed a normal decay mode up to a certain time, at which point, the curves exhibited a rapid decrease in count probability and a noticeable increase in statistical fluctuations. This effect is clearly demonstrated in Fig. 5. At approximately 3.0e-4 s, the statistical fluctuations increase and the apparent slope of the decay curve becomes much steeper (which cannot be a real effect). This effect is circumvented by performing the least-squares fit (LSF) on just the initial portion of the die-away curve.

Because the ^{3}He detectors used to perform the Rossi-α measurements were still operating at such high deadtimes, the *corrected* count rate at each of the subcritical configurations was assumed to be somewhat unreliable when estimating the alpha at delayed critical. Rather than plot the measured alphas as a function of the inverse of the corrected count rates from the ^{3}He detectors (i.e., the normal prodcedure), it was assumed that the low-efficiency fission chambers located in the two blankets would provide a more accurate estimate of the alpha at delayed critical since

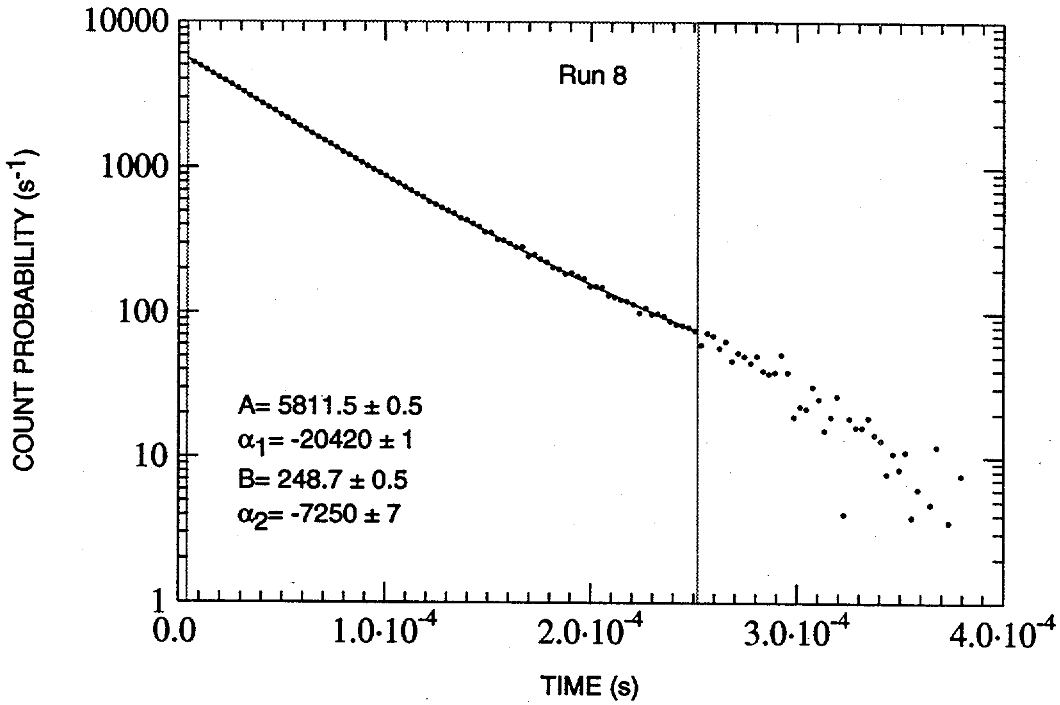

Fig. 5. Rossi-α curve at approximately -\$0.55. The data was accumulated for approximately 5 hours. The LSF was performed in the time interval between the origin and the vertical line drawn at 2.5e-4 s. The data to the right of the vertical line has been affected by the large intrinsic source strength.

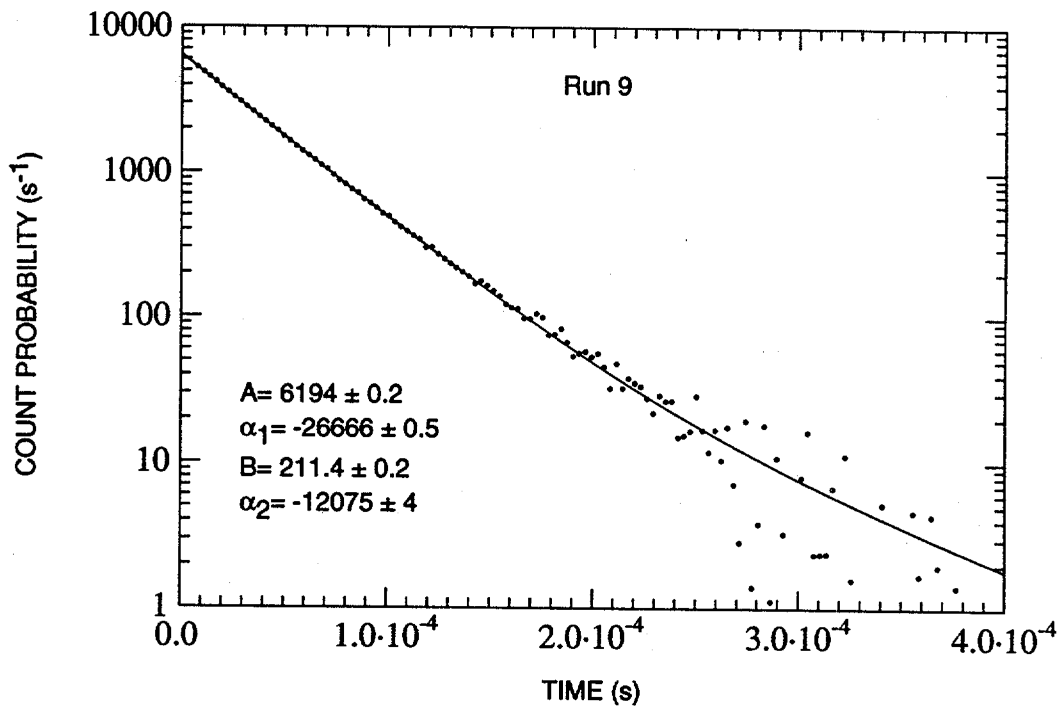

Fig. 6. Rossi-α curve at approximately -\$1.03. The data was accumulated for approximately 5 hours. The LSF was performed over the entire time interval. Unlike the Run 8, the effective intrinsic source strength at -\$1.02 is half of its value at –\$0.52. Hence, the later portion of the curve has not been distorted due to a short mean time between successive prompt fission chains.

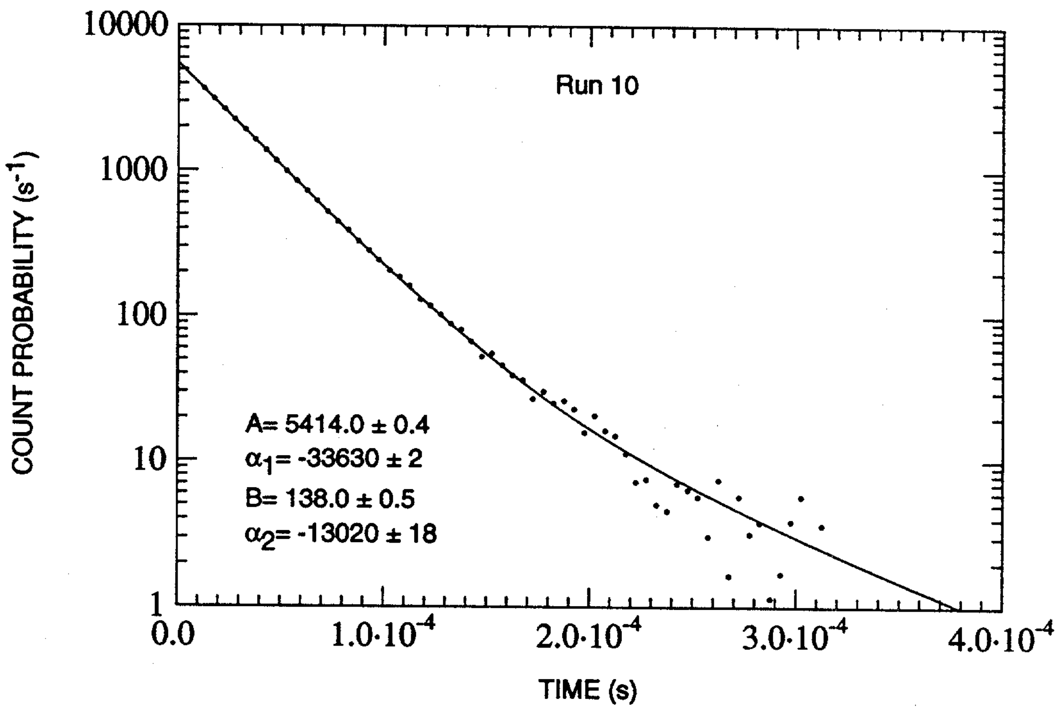

Fig. 7. Rossi-α curve at approximately -$1.56. The data was accumulated for approximately 5 hours. The LSF was performed over the entire time interval.

deadtime in those detectors would not be a factor. Using the data from all seven fission chambers, the rapid die-away alpha at each subcritical configuration was plotted as a function of the inverse count rate from each of the chambers. These data were then least-squares fit to a linear function to estimate the alpha at delayed critical for each chamber. A typical fit is shown in Figure 8. The results of the LSF for all of the chambers are summarized in Table II.

The average value of the y-intercept (i.e., the alpha at delayed critical) was obtained by taking a *weighted* average of the seven different intercepts obtained from the LSF. This yield a value of –1.31e4 +/- 134 (1σ) 1/s as the alpha at delayed critical *corresponding to the rapid die-away root.*

Based upon the final LSF of these data, the reactivity at each subcritical configuration was obtained by taking an average of the reactivity predicted at each subcritical configuration for all seven fission chambers. These results are listed in Table III.

Table II I.

Run #	Control Rod Positions	Rho ($)
8	129.99/130.00	–$0.553 +/- 0.014
9	206.02/206.03	–$1.031 +/- 0.021
10	305.00/305.00	–$1.558 +/- 0.024

(The uncertainties quoted in Table III represent the parent distribution error (1σ). The standard deviation about the mean, σ_m, would be a factor of $\sqrt{7}$ smaller since seven points were used to calculate the parent distribution error.)

A preliminary determination of the core neutron lifetime can be obtained using the calculated β_{eff} for this system as 0.0036 +/- 3% (1σ) and the measured alpha at delayed critical.

$$\tau_c = -\frac{\beta_{eff}}{\alpha_0} = \frac{-0.0036}{-13100} = 275 \text{ +/- } 3.2\% \text{ ns} \quad . \qquad (1)$$

(Once the measured value of β_{eff} is available, the prompt neutron lifetime for the *core* region will be reevaluated.) .

IV. CONCLUSIONS

At the risk of sounding somewhat melodramatic, this series of Rossi-α measurements is quite historic. To our knowledge, it is the first time that a Rossi-α experiment has been successfully performed in a system containing large amounts of plutonium. Usually, the intrinsic source strength is too high in most large plutonium systems to allow neutron noise measurements to be made. Our success stems from two facts. First, the large deadtime of the detector system was negated by running the correlator in the cross correlation mode and second, the neutron lifetime of the core was sufficiently small to allow prompt fission chains to be distinguished.

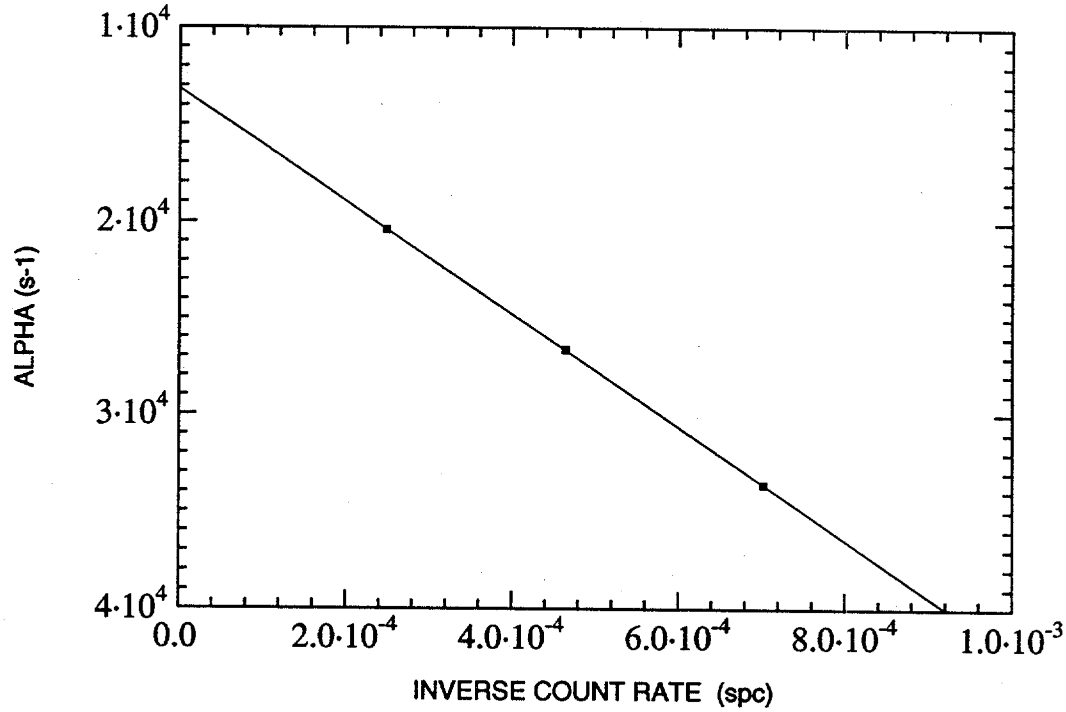

Fig. 8. Plot of the first (i.e., rapid) die-away time constant vs. the inverse of the count rate obtained by the M6 fission chamber located in the blanket region of the assembly. The alpha at delayed critical corresponds to 13150+/- 58 1/s.

TABLE II. LSF of Alpha Data for all Seven Fission Chambers

```
Least-squares fit of alpha vs. 1/C: M 1

  -12910.1       +/-       1.50E+02
  -140562.       +/-       1.41E+03 * x

      1/c          alpha-e        alpha-c         %diff          rho($)
  5.31463E-02   -20420.         -20380.        -.19402         -.57864
  9.84058E-02   -26666.         -26742.         .28522         -1.0714
   .14715       -33630.         -33593.        -.10933         -1.6021

Least-squares fit of alpha vs 1/C: M  2

  -13318.2       +/-        49.
  -148449.       +/-       4.99E+02 * x

      1/c          alpha-e        alpha-c         %diff          rho($)
  4.79317E-02   -20420.         -20434.       6.64882E-02   -.53426
  8.97424E-02   -26666.         -26640.      -9.61593E-02   -1.0003
   .13691       -33630.         -33642.       3.57739E-02   -1.5260

Least-squares fit of alpha vs 1/C: M  3

  -13081.4       +/-        8.9
  -464328.       +/-       2.78E+02 * x

      1/c          alpha-e        alpha-c         %diff          rho($)
  1.58100E-02   -20420.         -20422.       1.17919E-02   -.56118
  2.92466E-02   -26666.         -26661.      -1.70981E-02   -1.0381
  4.42595E-02   -33630.         -33632.       6.38801E-03   -1.5710

Least-squares fit of alpha vs 1/C: M  4

  -13177.7       +/-        33.
 -5.740405E+06   +/-       1.27E+04 * x

      1/c          alpha-e        alpha-c         %diff          rho($)
  1.26010E-03   -20420.         -20411.      -4.35769E-02   -.54892
  2.35266E-03   -26666.         -26683.       6.34696E-02   -1.0249
  3.56151E-03   -33630.         -33622.      -2.39216E-02   -1.5514
```

TABLE II. cont.

```
Least-squares fit of alpha vs 1/C: M  5

  -13202.1       +/-       53.
 -6.902150E+06   +/-      2.48E+04 * x

      1/c         alpha-e       alpha-c        %diff        rho($)
   1.04368E-03  -20420.       -20406.     -7.03408E-02  -.54564
   1.95465E-03  -26666.       -26693.       .10256      -1.0219
   2.95779E-03  -33630.       -33617.     -3.87404E-02  -1.5464

Least-squares fit of alpha vs 1/C: M  6

  -13149.5       +/-       54.
 -2.917213E+07   +/-      1.07E+05 * x

      1/c         alpha-e       alpha-c        %diff        rho($)
   2.48725E-04  -20420.       -20405.     -7.19212E-02  -.55180
   4.64296E-04  -26666.       -26694.       .10496      -1.0300
   7.01607E-04  -33630.       -33617.     -3.96820E-02  -1.5565

Least-squares fit of alpha vs 1/C: M  7

  -13166.8       +/-       61.
 -3.191998E+07   +/-      1.31E+05 * x

      1/c         alpha-e       alpha-c        %diff        rho($)
   2.26716E-04  -20420.       -20404.     -8.05522E-02  -.54962
   4.23890E-04  -26666.       -26697.       .11765      -1.0276
   6.40615E-04  -33630.       -33615.     -4.45413E-02  -1.5530

Average Intercept =  -13099.3 +/-   134.043

Average values of Rho +/- sig :
 -.552867 +/-   1.389848E-02
 -1.03061 +/-   2.144045E-02
 -1.55807 +/-   2.359724E-02
```

In future experiments in large plutonium systems, some improvements in the data acquisition system can be obtained by increasing the overall efficiency of the detector system. This can be accomplished by using more detectors. Using more detectors will also increase our ability to better resolve the second (and third?) slower die-away time constant that may be present due to a reflector.

V. ACKNOWLEDGEMENT

We would like to thank the reactor operators—Mr. Hayasaka, Mr. Kurosawa, Mr. Sodeyama, and Mr. Satoh—and the FCA technical staff for their support during the performance of this experiment. And, we would also like to thank Dr. Nakagawa, Director of Reactor Engineering, and Mr. Osugi, Chief of the FCA facility, for their continued support of this international project.

Appendix A
Preliminary Results

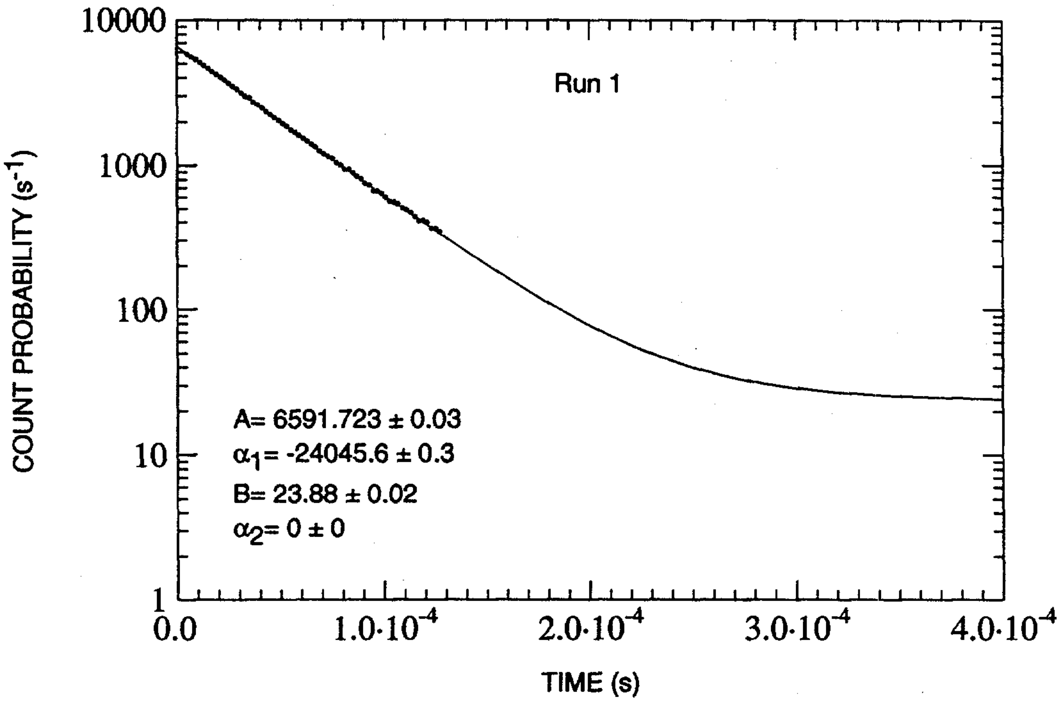

Fig. A-1. Rossi-α curve at approximately -\$0.82. The second decay constant could not be resolved since the time scale of the measurement was too short. However, it was apparent that the curve did not follow a simple exponential as evidenced by the small background that was needed to remove trends in the residuals of the least squares fit.

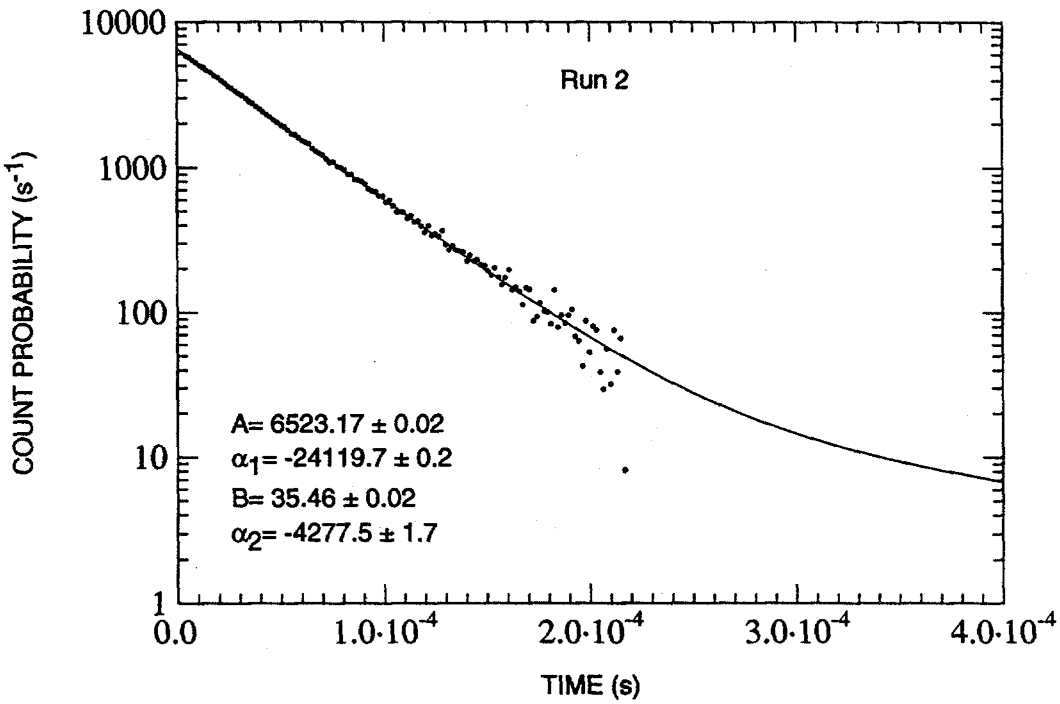

Fig. A-2. Rossi-α curve at approximately -$0.82. The time scale for this run was nearly doubled relative to the time scale used in Run 1. As a result, the second decay constant was resolvable.

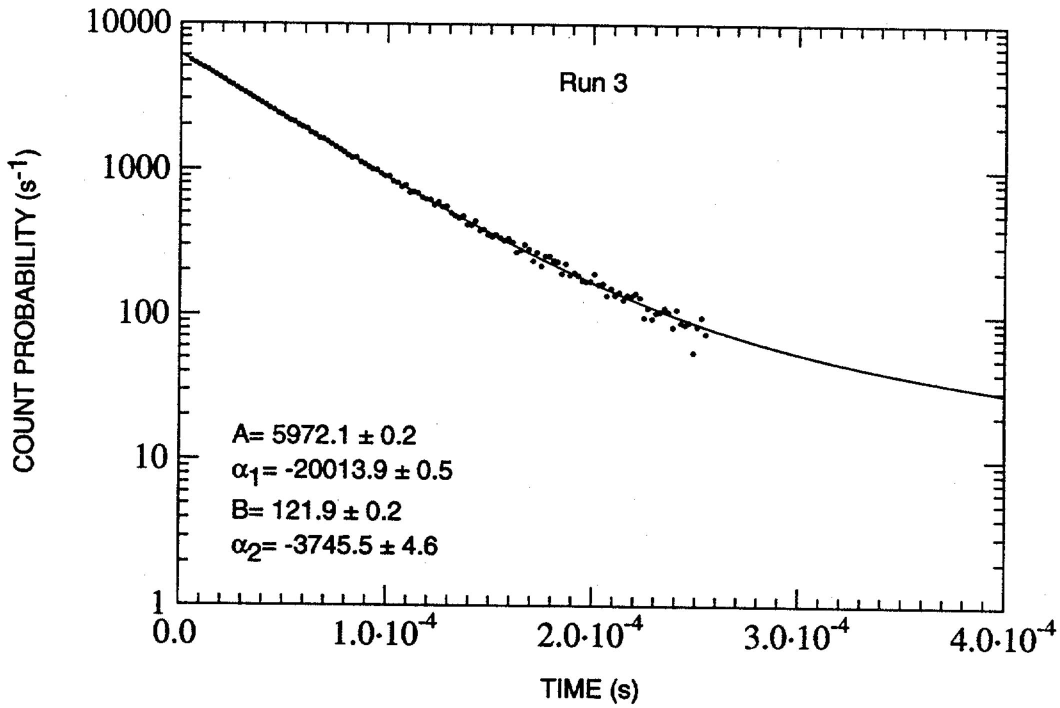

Fig. A-3. Rossi-α curve at approximately -$0.52.

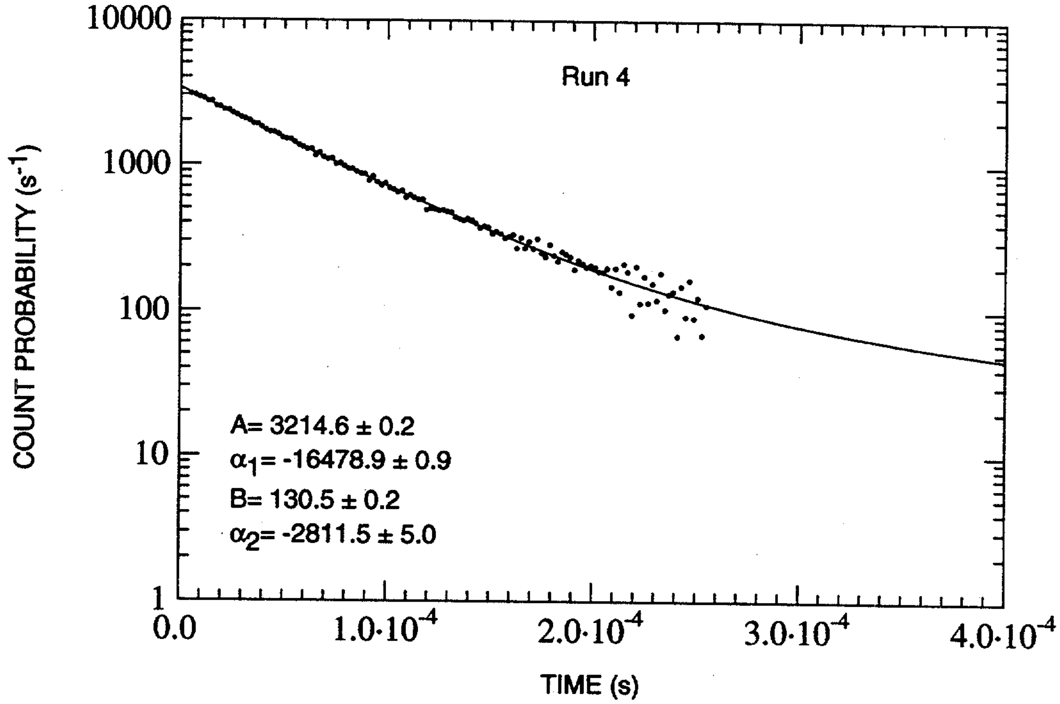

Fig. A-4. Rossi-α curve at approximately -$0.25. The detector system was very nearly saturated during this run. The effective deadtime was estimated to be approximately 25% for each pair of detectors. Hence, each detector was operating at approximately 50% deadtime. Nevertheless, both alphas were resolvable, and the reactivity determine from these data was consistent with the reactivity determined using a control rod calibration

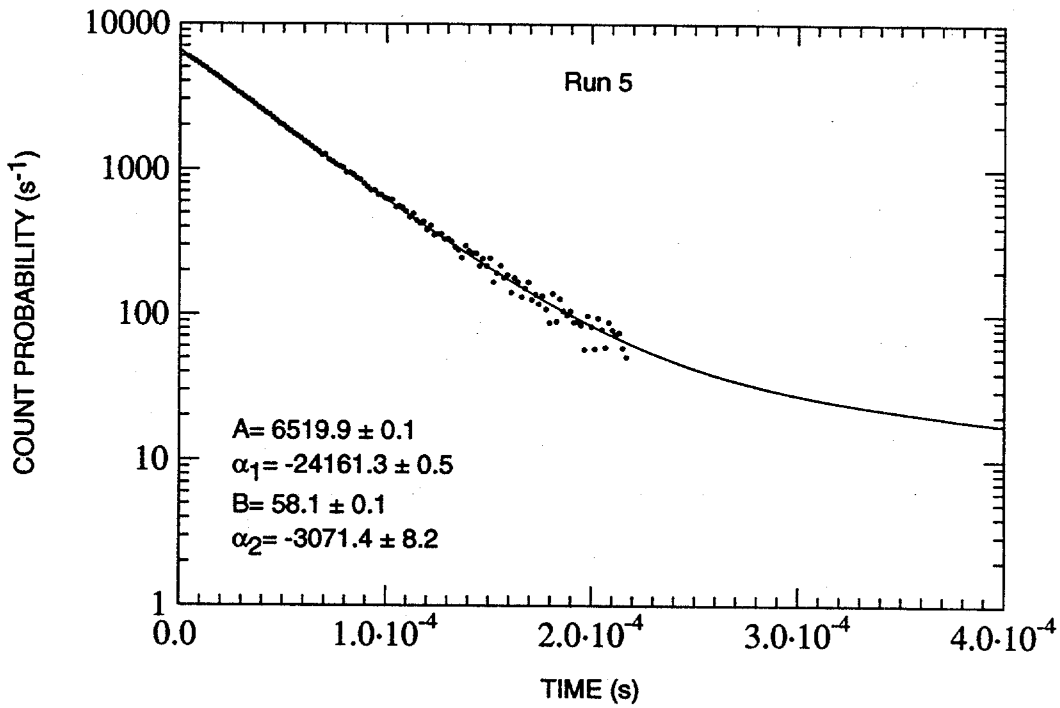

Fig. A-5. Rossi-α curve at approximately -\$0.82. This was a repeat of Run 1.

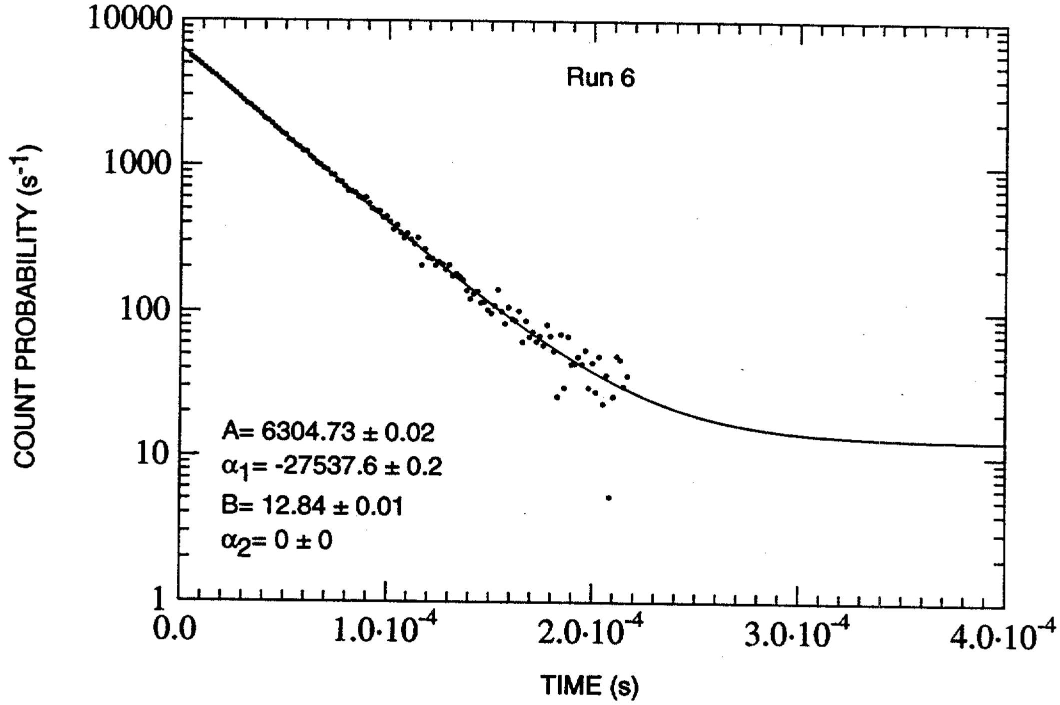

Fig. A-6. Rossi-α curve at approximately -\$1.08. As with Run 2, we were unable to resolve the second decay constant since the time span of the measurement was too short.

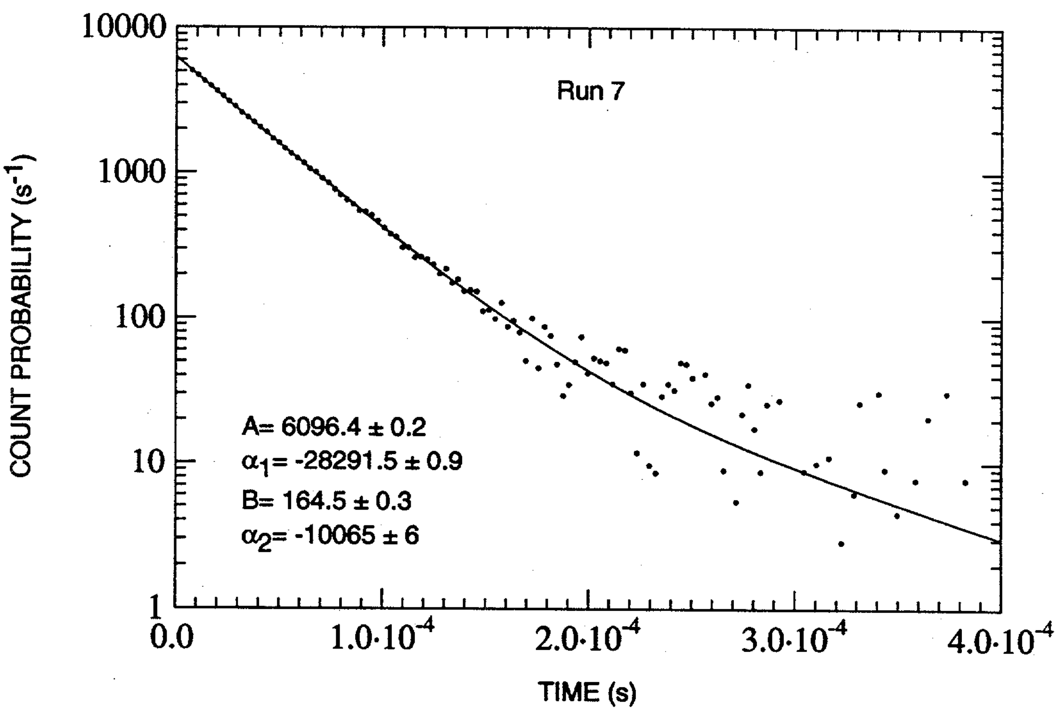

Fig. A-7. Rossi-α curve at approximately -\$1.15. The time scale was increased to allow the second time constant to be resolved. However, the statistics are very poor indicating that the run time needs to be increased.

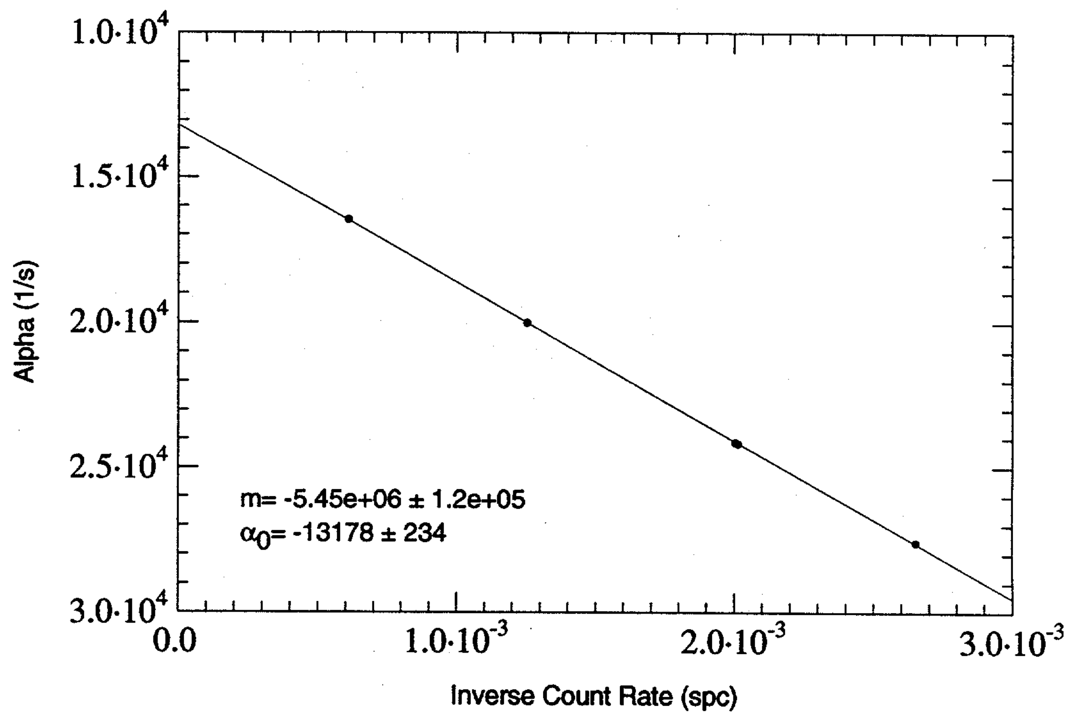

Fig. A-8. Plot of first prompt decay alphas (from preliminary runs 1 through 7) vs. inverse count rate obtained from low-efficiency fission chamber (M4) located in depleted blanket of assembly. [Note, there were three data points taken at -$0.82 (i.e., 2.0e-03 spc). The uncertainty of each alpha is less than the size of the symbol in the above figure (see Figs. A-1 through A-7). By extrapolating to zero, α_0 was determined to be 1.32e+04 (1/s). Assuming a β_{eff} of 0.0036, the core neutron lifetime corresponds to approximately 273 ns.]